Simulations of the output of the Ne-like Ti x-ray laser at 32.6 nm driven by the grazing-incidence pumping scheme

J. Zhao, Q. L. Dong, F. Yan, and J. Zhang*

Laboratory of Optical Physics, Institute of Physics, Chinese Academy of Sciences, Beijing 100080

(Received 10 January 2006; published 23 March 2006)

Numerical simulations are presented for the output of a Ne-like Ti soft x-ray laser at 32.6 nm driven by the grazing-incidence pumping (GRIP) scheme, using a modified one-dimensional (1D) lagrangian hydrodynamic code MED103 coupled with an atomic physics data package and a 2D RAYTRACE code as a postprocessor. We predict that saturation can be achieved at a plasma length of 0.2 cm by an optimized driving configuration with an energy of only 200 mJ. We also compare the output beam quality of the Ne-like Ti soft x-ray laser generated by an optimized pump energy of 200 mJ and a higher energy of 385 mJ. Better spatial coherence is expected for a higher pump energy.

DOI: 10.1103/PhysRevA.73.033816 PACS number(s): 42.55.Vc, 42.60.By, 52.50.Jm

I. INTRODUCTION

Since the first demonstration of Neon-like x-ray lasers at about 20 nm in 1984 by using Kilo Joule lasers, great efforts have been made to improve efficiency and reduce the driving energy of x-ray lasers. A number of techniques have been developed including multiple pumping pulses and double targets [1–5], curved targets [6,7]. The driver energy requirements have been dramatically reduced to a few joules by application of the transient collisional excitation scheme [8,9]. Recently the driven energy for the transient collisional excited soft x-ray lasers has been further reduced using the grazing-incidence pumping (GRIP) scheme. In this scheme a main driven pulse irradiates a preplasma at an optimized incidence angle and is refracted into the gain region. This significantly increases the energy deposition into this region. Furthermore, it is an inherent traveling wave pump very close to the speed of light. Using this scheme the saturated Ni-like Mo soft x-ray laser at 18.9 nm was demonstrated with a pump energy as small as 150 mJ [10]. To date this GRIP scheme has been successfully applied to many Ne-like or Ni-like ions. High repetition rate opteration of saturated soft x-ray lasers have been demostrated in the $2p^5 3p\ ^1S_0 \rightarrow 2p^5 3s\ ^1P_1$ transitions of Ne-like ions Ti ($Z=22$), V ($Z=23$) at 32.6 nm, 30.4 nm and also in the 4d $^1S_0 \rightarrow 4p\ ^1P_1$ transitions of Ni-like ions Ru ($Z=44$), Pd ($Z=46$), Ag ($Z=47$), Cd ($Z=48$) at 16.5, 14.7, 13.9, and 13.2 nm [10–13]. Strong lasing approaching gain saturation was observed at 11.9 nm for the Ni-like Sn ($Z=50$) x-ray laser [12]. The grazing-incidence pumped Ni-like Mo x-ray laser at 18.9 nm has been demonstrated by many groups using different drive pulse configurations with very different pump energies [10,14,15].

In this paper we numerically investigate a transient collisional Ne-like Ti x-ray laser at 32.6 nm using the grazing-incidence pump scheme. A modified version of the one-dimensional (1D) Lagrangian hydrodynamic code MED103 coupled with an atomic physics data package is used to predict the time evolution of the laser-plasma interactions and gain coefficients. This code has been used to predict the grazing-incidence pumped Ni-like Mo experiment successfully [16]. A 2D ray-tracing code is developed to calculate the variation of the output intensity of x-ray lasers versus the plasma length. The refraction effects in the radial direction and saturation effects are taken into account. Using this code we can reproduce the main results of the experiments done by Alessi *et al.* [11], where double prepulses followed by a 8 ps main pulse were used to pump the Ne-like Ti soft x-ray laser and the total pump energy was about 1.36 J.

II. PREPLASMA CONDITIONS FOR THE GRIP X-RAY LASERS

The conditions of the plasma just before the onset of the main pulse are crucial for strong x-ray laser action. It is well known that for the collisional pump Ne-like x-ray lasers, the prepulse(s) should make the population on the ground state of the Ne-like ions in the preplasma as high as possible. The density gradient in the plasma must be sufficiently shallow to prevent significant refraction of the x-ray laser beam. The difference from the traditional tranverse pump is that for the GRIP scheme x-ray lasers, the short main pump pulse irradiates into the preplasma at a grazing incidence angle. The main pump pulse with an initial incidence angle (θ) turns back into the preplasma at the density $n_e = n_c \sin^2(\theta)$, where $n_c \simeq 1.1 \times 10^{21}\ /\lambda^2(\mathrm{cm}^{-3})$ is the critical density for the wavelength of the pump laser. For each specific soft x-ray laser of Ne-like or Ni-like ions there is a desired electron density for laser gain [17]. The energy of the main pulse should be efficiently absorbed in the gain region, if there is a spatial matching of the gain region and the refraction point in the preplasma. For low and middle Z elements, like titanium, it is easy to maintain a high fraction of Ne-like ions for a long time. It is also easy to satisfy the optimum plasma conditions required for the GRIP Ne-like Ti soft x-ray lasers simultaneously. Later in this paper we will apply different drive configurations to find an optimized drive conditions for the GRIP Ne-like Ti x-ray laser.

*Electronic address: jzhang@aphy.iphy.ac.cn

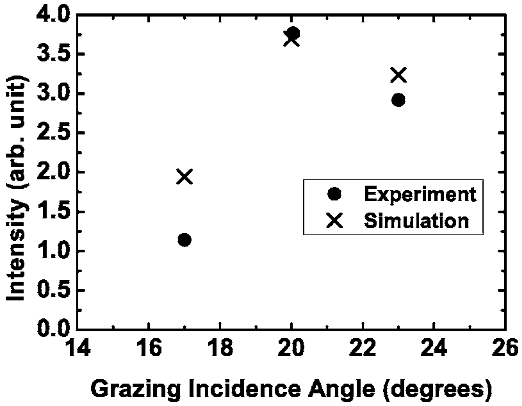

FIG. 1. Numerical simulation and experimental results of the output intensity of the Ne-like Ti x-ray lasers at three grazing incidence angles of 17°, 20°, and 23°.

III. SIMULATION OF A TYPICAL EXPERIMENT

First of all, using our modified 1D Med103 and 2D raytracing code we try to reproduce the experiment done by Alessi *et al.* [11]. The wavelength of the pump laser is 800 nm. The pump geometry is set to be the standard line focus on a 100 μm—*thick* slab target. All pulses are in a Gaussian profile. Two uncompressed laser prepulses (120 ps duration) with an interval about 5 ns are used to form a plasma by irradiating the target at normal incidence. Their intensities are 2.37×10^{12} and 6.77×10^{10} W/cm^2, respectively. A 8 ps main pulse with an intensity of 1.0×10^{14} W/cm^2 is used to rapidly heat the preplasma at a selected grazing incidence angle onto the plasma. Figure 1 gives the simulation and experimental [11] results of the output intensity of x-ray lasers at three grazing incidence angles of 17°, 20°, and 23°, which were adopted in the experiment [11]. The optimized delay time between the main prepulse and the short pulse for a grazing incidence angle of 20° is also simulated and found to be 600 ps for the Ne-like Ti ions. This proves that this modified code can reproduce the experimental results of grazing-incidence Ne-like Ti soft x-ray lasers.

IV. OPTIMIZATION OF DOULE PULSE PUMPING SCHEME

The drive configuration with double prepulse is complicated to control the parameters in soft x-ray laser experiments. So we try to simplify this to a prepulse pump scheme, in which one prepulse followed by a short main pulse. In order to observe the influence of the prepulse durations on the final output of the Ne-like Ti x-ray lasers, two different duration of 300 ps and 1 ns full width at half maximum are applied. The duration of the main short pulse is fixed to be 300 fs for the transient collisional pump scheme. To find the minimum energy necessary to pump saturated soft x-ray lasers, optimizations are performed in terms of the peak intensity of the prepulse, the delay time between the prepulse and the short main pulse, the peak intensity and the incidence angle of the main pulse.

The optimized peak intensity for a 300 ps and a 1 ns prepulse to get a high fraction of Ne-like ions without overi-

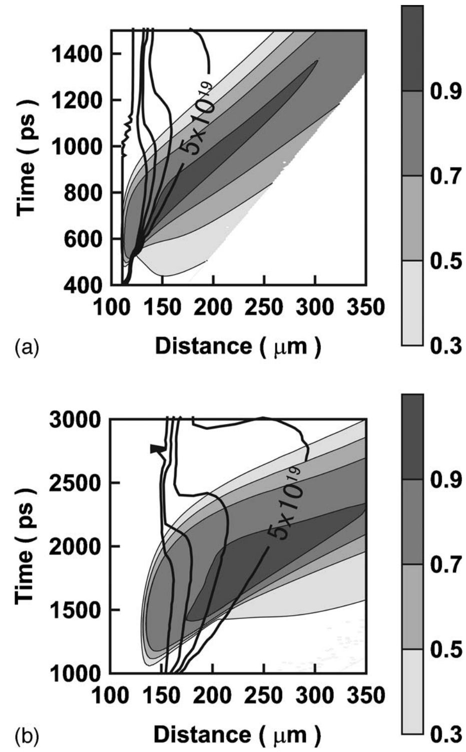

FIG. 2. Spatiotemporal profile of the ground state Ne-like ions fraction and the electron density in the plasma for (a) a 300 ps prepulse with a peak intensity of 4×10^{11} W/cm^2 and (b) a 1 ns prepulse with a peak intensity of 2.5×10^{11} W/cm^2. The fraction of the Ne-like Ti ions is depicted by a grey scale from 30% (white) to 90% (black). The electron density is described only by lines with further inside a step of 5×10^{19} cm^{-3}. The outmost line indicates the electron density of 5×10^{19} cm^{-3}.

onization, is found to be 4×10^{11} and 2.5×10^{11} W/cm^2, respectively. Figure 2 gives the spatiotemporal profile of the ground state Ne-like ions fraction and the electron density distributions in the plasma for (a) a 300 ps prepulse with an optimized peak intensity of 4×10^{11} W/cm^2 and (b) a 1 ns prepulse with an optimized peak intensity of 2.5×10^{11}W/cm^2, respectively. The horizontal axis presents the spatial distance in the direction of plasma expansion. The peak time of those two prepulses are set to be 540 and 1200 ps. The fraction of Ne-like Ti ion is depicted by a grey scale ranging from 30% (white) to 90% (black). High fraction of Ne-like ions can be maintained for over 500 ps. The electron density is described only by lines with further inside consecutive steps of 5×10^{19} cm^{-3}. The outmost line indicates the electron density of 5×10^{19}cm^{-3}and the most inside line indicates the desired electron density of 2×10^{20} cm^{-3} for the Ne-like Ti x-ray laser. The critical surface at the density of 1.72×10^{21} cm^{-3} is located at 110 and 125 μm respectively. The 1 ns prepulse in Fig. 2(b) has shown a much more spatially extended Ne-like ions distribution and a low electron density gradient.

With the optimized prepulses a main pulse with a peak intensity of 3×10^{14} W/cm^2 is turned on and irradiated into the preplasmas at an incident angle of 20° which is an optimized incidence angle in the experiment [11]. The optimized delay time between the prepulse and the main pulse is found

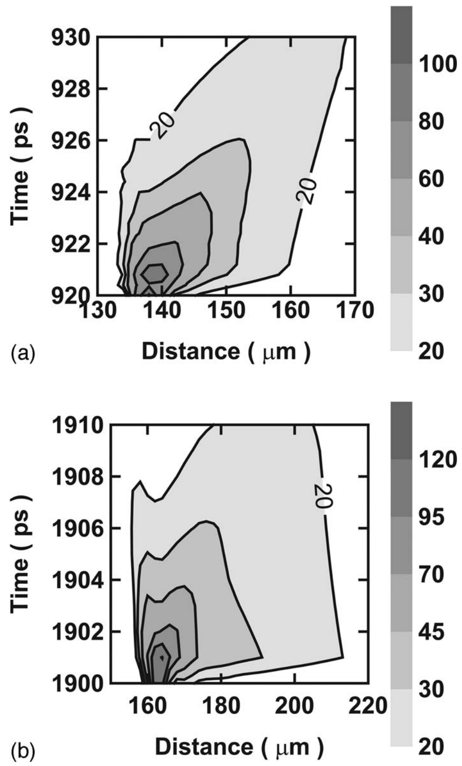

FIG. 3. Coutours for the Ne-like Ti gain versus space and time for (a) a 300 ps prepulse and (b) a 1 ns prepulse. The gain is depicted by the grey scale besides in a unit of cm^{-1}.

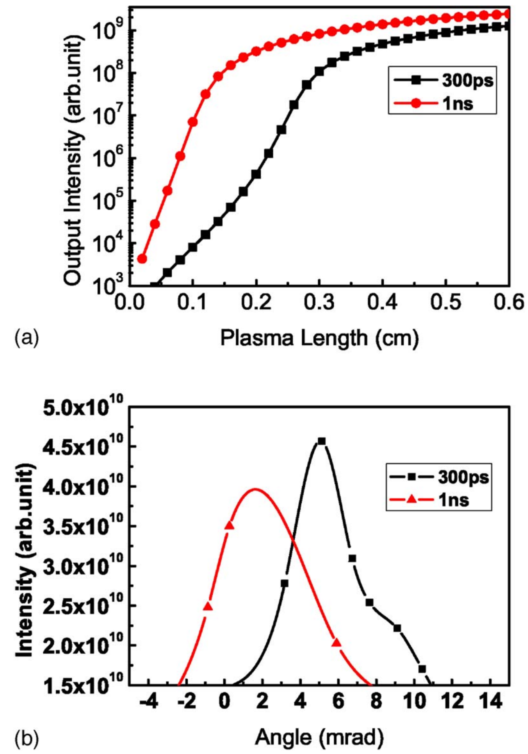

FIG. 4. (Color online) Ray-tracing results of the output of x-ray laser intensity versus (a) the plasma length and (b) the angular distribution at the saturated plasma length of 0.36 and 0.2 cm for the two drive configurations, 300 ps and 1 ns prepulse.

to be 380 and 700 ps for the two prepulses respectively. Figure 3 shows the coutours of the gain coefficient versus space and time for (a) the 300 ps prepulse and (b) the 1 ns prepulse with the optimized delay time. The maximum local gain coefficient for each prepulse is 100 versus 140 cm^{-1}. We can see the gain extent for the 1 ns prepulse case is almost twice as wide as in the case with a 300 ps prepulse. After ray-tracing post-processing Fig. 4 gives the output of the soft x-ray laser intensity versus (a) the plasma length and (b) the anglar distribution for both prepulses. Saturation is achieved at a plasma length of 0.36 and 0.2 cm for the 300 ps prepulse and the 1 ns prepulse. If the focal width is assumed to be 30 μm and the pump energies are 227 and 204 mJ, respectively. Because of the low electron density in the plasma generated by the 1 ns prepulse, the corresponding output has a better beam quality as shown in Fig. 4(b). So the drive configuration with a nanosecond prepulse is favorable for a better beam quality of the GRIP Ne-like Ti soft x-ray lasers.

The peak intensity and the grazing incidence angle of the main pulse are also optimized for the 1 ns prepulse. Figure 5 gives the ray-tracing results of the output of the soft x-ray laser intensity versus the plasma length for short main pulses (a) with different peak intensities from 1×10^{14} to 4×10^{14} $\mathrm{W/cm^2}$ at an incident angle of 20° and (b) at different incident angles with a peak intensity of 3×10^{14} $\mathrm{W/cm^2}$. It is obvious that the optimum intensity of the main pulse is 3×10^{14} $\mathrm{W/cm^2}$ which provides saturation with a shortest plasma length, corresponding to a minimum pump energy. From Fig. 5(b) at the optimum incidence angle of 20° the pump beam is refracted at an electron density of about 2×10^{20} $\mathrm{W/cm^2}$ where is the gain region of the Ne-like Ti soft x-ray laser. It significantly helps increase energy absorption of the pump beam in the gain region. It is also easy to understand that at some steeper incidence angle of 23° and 25°, most of the beam energy is absorbed in a higher electron density away from the gain region and has a steeper gradient which is disadvantageous for amplification of x-ray lasers.

The optimized prepulse pump scheme is found to be a normal incident 1 ns prepulse with a peak intensity of 2.5×10^{11} $\mathrm{W/cm^2}$, followed by a 300 fs main pulse with a peak intensity of 3×10^{14} $\mathrm{W/cm^2}$ at an incidence angle of 20°. Saturation can be achieved at a plasma length of 0.2 cm. The pump energy is about 204 mJ which is much less than the energy used in the experiment. Saturated operation of Ne-like Ti x-ray lasers can be demostrated using relatively small laser system.

V. COMPARISON OF OPTICAL QUALITY OF THE OUTPUT OF X-RAY LASERS

For those demonstrated grazing incidence pumped Ni-like Mo x-ray lasers, different pump energies ranging from ~150 mJ to ~1.3 J, were used in experiments [10,14,15]. Here we try to introduce a higher pump energy to grazing incidence Ne-like Ti soft x-ray lasers. A 1 ns prepulse with a higher peak intensity of 3.5×10^{11} $\mathrm{W/cm^2}$ is applied to irradiate on the target at normal incidence. An over-ionized preplasma is induced, which results in higher electron tempera-

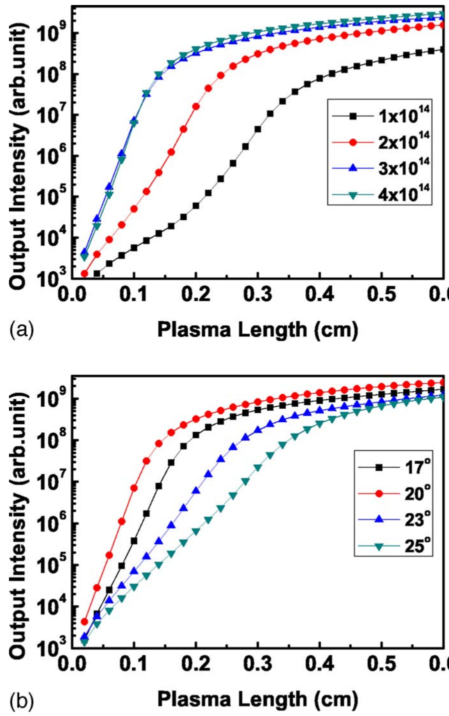

FIG. 5. (Color online) Ray-tracing results of the output of x-ray laser intensity versus plasma length for main pulses (a) with different peak intensities from 1×10^{14} to 4×10^{14} W/cm^2 at an optimum incident angle of 20° and (b) at different incidence angles from 17° to 25° with an optimum peak intensity of 3×10^{14} W/cm^2.

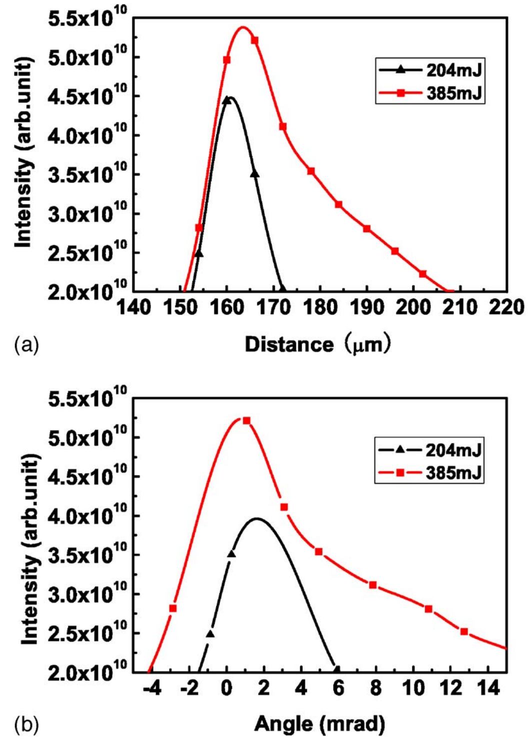

FIG. 6. (Color online) The output of the 32.6 nm x-ray laser intensity versus (a) the source position and (b) the anglar distribution for two pump cases with the optimized energy of 204 mJ and a higher energy of 385 mJ.

ture, prevents Ne-like ion population decreasing through electron-ion recombination after longer time delay between pre- and main pulses and generates much smoother electron density profile. After an optimum delay time of 800 ps, a 1.5 ps short pulse with a peak intensity of 1×10^{14} W/cm^2 is irradiated into the plasma at a grazing incidence angle of 20°. Saturation is achieved at a plasma length of 0.25 cm. Assuming that the target is 30 μm wide, the related total pump energy is then about 385 mJ. Using the 2D ray-tracing code, the beam quality of the anglar distribution (far field) and the source position (near field) of the output of soft x-ray lasers at the end of the target are recorded. Figure 6 gives the output of the 32.6 nm x-ray laser intensity versus (a) the source position and (b) the anglar distribution for two pump cases with optimized energy of 204 mJ and higher energy of 385 mJ. Here we can see using a higher pump energy, which causes overionization in the plasma, can reduce refraction, produce a smaller tilt angle ~1 mrad, and a higher output intensity of x-ray lasers. So higher pump energy is required if high beam quality of x-ray laser is expected.

VI. CONCLUSION

Numerical simulations are presented for the output of the grazing incidence pumping Ne-like Ti soft x-ray laser at 32.6 nm. We simplify the double prepulse drive configuration used in the experiment to a prepulse pump scheme which is much easy to control for practical experiments. Optimizations are performed in terms of the peak intensity of the prepulse, the delay time between the two pulses, the peak intensity, and the incidence angle of the main pulse. Saturation can be achieved at a plasma length of 0.2 cm by the optimized drive configuration with an energy about 200 mJ. Better beam quality of the output of the Ne-like Ti soft x-ray laser can be obtained using a higher pumping energy of 385 mJ.

ACKNOWLEDGMENTS

This work is jointly supported by the National Natural Science Foundation of China (under Grant No. 10474137, No. 60478047, and No. 60321003) and the National HI-tich ICF Programe.

[1] M. D. Rosen, *OSA Proc. on Short-Wavelength Coherent Radiation: Generation and Applications*, Vol. 11, edited by P. Bucksbaum and N. Ceglio (Optical Society of America, Washington, D.C. 1991), p. 73.
[2] L. B. Da Silva, B. J. MacGowan, D. L. Matthews, M. D. Rosen, H. A. Baldis, G. D. Enright, B. LaFontaine, and D. M. Villeneuve, Proc. SPIE **1229**, 128 (1990).
[3] J. A. Plowes, G. J. Pert, and P. B. Holden, Opt. Commun. **116**, 260 (1995).
[4] S. B. Healy, G. F. Cairns, C. L. S. Lewis, G. J. Pert, and J. A. Plowes, IEEE J. Sel. Top. Quantum Electron. **1**, 1156 (1995).
[5] G. F. Cairns, C. L. S. Lewis, M. J. Lamb, A. G. MacPhee, D. Neely, P. Norreys, M. H. Key, S. B. Healy, P. B. Holden, G. J. Pert, *et al.*, Opt. Commun. **123**, 777 (1996).
[6] J. G. Lunney, Appl. Phys. Lett. **48**, 891 (1986).
[7] R. Kodama, D. Neely, Y. Kato, H. Daido, K. Mural, G. Yuan, A. MacPhee, and C. L. S. Lewis, Phys. Rev. Lett. **73**, 3215 (1994).
[8] P. J. Warwick, C. L. S. Lewis, M. P. Kalachnikov, P. V. Nickles, M. Schnurer, A. Behjat, A. Demir, G. J. Tallents, D. Neely, and E. Wolfrum, J. Opt. Soc. Am. B **15**, 1808 (1998).
[9] M. P. Kalachnikov, P. V. Nickles, M. Schnurer, W. Sandner, V. N. Shlyaptsev, C. Danson, D. Neely, E. Wolfrum, J. Zhang, A. Behjat, *et al.*, Phys. Rev. A **57**, 4778 (1998).
[10] R. Keenan, J. Dunn, P. K. Patel, D. F. Price, R. F. Smith, and V. N. Shlyaptsev, Phys. Rev. Lett. **94**, 103901 (2005).
[11] D. Alessi, B. M. Luther, Y. Wang, M. A. Larotonda, M. Berrill, and J. J. Rocca, Opt. Express **13**, 2093 (2005).
[12] J. J. Rocca, Y. Wang, M. A. Larotonda, B. M. Luther, D. Alessi, M. Berrill, A. Weith, M. C. Marconi, C. S. Menoni, and V. N. Shlyaptsev, Soft X-Ray Lasers and Applications VI **5919**, 591901 (pages 12) (2005).
[13] J. Dunn, R. Keenan, and V. N. Shlyaptsev, Soft X-Ray Lasers and Applications VI **5919**, 591905 (pages 8) (2005).
[14] J. Tummler, K. A. Janulewicz, G. Priebe, and P. V. Nickles, Phys. Rev. E **72**, 037401 (2005).
[15] B. M. Luther, Y. Wang, M. A. Larotonda, D. Alessi, M. Berrill, M. C. Marconi, J. J. Rocca, and V. N. Shlyaptsev, Opt. Lett. **30**, 165 (2005).
[16] F. Yan, J. Zhang, Q. L. Dong, X. Lu, and Y. J. Li, Phys. Rev. A **73**, 023812 (2006).
[17] H. Daido, S. Ninomiya, T. Imani, Y. Okaichi, M. Takagi, R. Kodama, H. Takabe, Y. Kato, F. Koike, J. Nilsen, *et al.*, Int. J. Mod. Phys. B **11**, 945 (1997).